RSC Advances

ROYAL SOCIETY
OF CHEMISTRY

www.rsc.org/advances
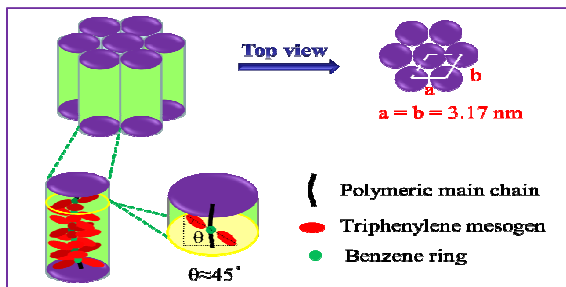
Highlight

➢ Phase Behavior of Mesogen-Jacketed Liquid Crystalline Polymer with Triphenylene Discotic Liquid Crystal Mesogen Unit

PAPER

Synthesis and Phase Behavior of Mesogen-Jacketed Liquid Crystalline Polymer with Triphenylene Discotic Liquid Crystal Mesogen Unit in Side Chains

Jianfeng Ban, Sheng Chen, Hailiang Zhang*

A novel Mesogen-Jacketed Liquid Crystalline Polymer (MJLCP) containing two triphenylene (Tp) units in the side chains, named poly[bis(3, 6, 7, 10, 11-pentakis (hexyloxy) triphenylen-2-yl)2-vinylterephthalate] (PBTCS), was designed and successfully synthesized via conventional free radical
10 polymerization. The chemical structure of the monomer was confirmed by ^{1}H/^{13}C NMR, and high-resolution mass spectrometry. The molecular characterization of the polymer was performed with ^{1}H NMR, gel permeation chromatography (GPC) and thermogravimetric analysis (TGA). The phase structure and transition of the polymer were investigated by the combination of techniques including differential scanning calorimetry (DSC), polarizing optical microscope (POM), 1D/2D wide-angle X-ray
15 diffraction (1D and 2D WAXD) and 1D Small-angle X-ray scattering (1D SAXS), respectively. The results showed that the PBTCS got a relatively high glass transition temperature and formed a higher symmetry hexagonal columnar (Φ_H) phase due to the strong coupling effect between the Tp moieties and the MJLCP main chain.

Introduction

20 Polymeric discotic liquid crystals (DLCs) have attracted great attention because of their capability of self-assembling into well different ordered structures, lead to producing the interesting physical properties, which can be applied such as in optical compensation films, one-dimensional conductor, anisotropic
25 photoconductors, and photovoltaic solar cells.[1-15] DLCs were first realized by the Ringsdorf et al.[16] and subsequently many kinds of discotic polymers have been prepared. Among them, the phase behavior and phase structure of end-on side chain liquid crystal polymers (SCLCPs) containing triphenylene (Tp) derivatives
30 with long flexible spacer as linkers have been widely investigated.[15,17-20] The research shows that this kind of SCLCPs can self-organize into well-ordered, self-healable supramolecular columns due to the π - π stacking of the planar aromatic cores and the van der Waals interactions of the peripheral chains. For
35 example, poly(meth) acrylates, polysiloxanes and polyacetylenes containing Tp moieties in the side chains.[21-27]

Mesogen-jacketed liquid crystalline polymers (MJLCPs) have been systematically studied during the past two decades because they display many special properties, which is similar to the rigid
40 backbone polymers, such as high glass transition temperature, broad temperature range of mesophase, long persistence length in good solvent, and forming banded texture after mechanical shearing in LC state.[28-35] MJLCPs is a side-on side-chain liquid crystalline polymers, in which the bulky side-chain mesogens are
45 side-on attached to the flexible main chain through a short spacer or a single covalent. Owing to the strong steric effect, many MJLCPs show columnar phases in which each cylinder is formed by a single MJLCP chain molecule. Recently, a series of MJLCPs containing two triphenylene (Tp) units with different lengths of
50 the methylene units between the terephthalate core and Tp moieties in the side chains have been prepared by Zhu et al. and the phase behaviors of these combined main-chain/side-chain liquid-crystalline (LC) polymers were investigated.[36,37] The results indicated that individual ordered structures developed at
55 the different temperature by these two LC building blocks were not only competitive but also promotive to each other.

Interesting point arises concerning the properties of MJLCPs when the Tp moieties are direct connected to main chain. Of particular interest is to ask in whether "jacketed-effect" has
60 influence on the π - π stacking of the Tp mesogen. So, in this paper, we design and synthesize a novel MJLCP with Tp DLCs as the mesogens unit which is direct connected to the repeating unit of the poly(vinyl terephthalate) main chain without flexible spacer. The target polymer PBTCS is shown in Chart 1. In this
65 work, the phase transitions and structures of PBTCS have been studied in detail. To the best of our knowledge, this is the first

Key Laboratory of Polymeric Materials and Application Technology of Hunan Province, Key Laboratory of Advanced Functional Polymer Materials of Colleges, Universities of Hunan Province, College of Chemistry, Xiangtan University, Xiangtan 411105, Hunan Province, China. Email: huaxuechensheng@163.com, zhl1965@xtu.edu.cn

report of MJLCP with discotic mesogens direct connected to the main chain without flexible spacer. The polymer exhibiting extraordinary stabilized hexagonal columnar structures, which could guide the design of ordered functional LC polymers bearing discotic mesogens.
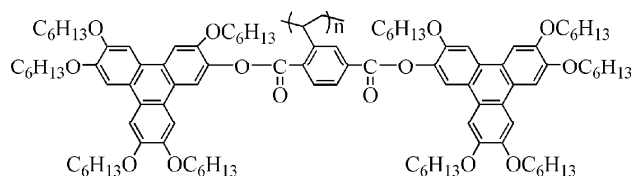
Chart 1 Chemical structure of PBTCS

Experimental

Materials

The precursor 2-vinylterephthalic acid (VTA) was synthesized according to previous paper.[38] Anhydrous tetrahydrofuran (THF) was distilled from sodium benzophenone ketyl under argon and used immediately. 2, 2-Azobisisobutyronitrile (AIBN) was freshly recrystallization from methanol. Dichloromethane (CH_2Cl_2) was dried over magnesium sulfate anhydrous. All other reagents and solvents were used as received without further purification.

Instruments and measurements

Nuclear magnetic resonance (NMR). $^1H/^{13}C$ NMR measurements were performed on a Bruker ARX400 MHz spectrometer using with $CDCl_3$ as solvent, tetramethylsilane (TMS) as the internal standard at ambient temperature. The chemical shifts were reported on the ppm scale.

Gel permeation chromatography (GPC). The apparent number average molecular weight (M_n) and polydispersity index (PDI = M_w/M_n) were measured on a GPC (WATERS 1515) instrument with a set of HT3, HT4 and HT5. The μ-styragel columns used THF as an eluent and the flow rate was 1.0 ml min^{-1} at 38 ^{o}C. The GPC data were calibrated with polystyrene standards.

Thermogravimetric analysis (TGA). TGA was performed on a TA SDT 2960 instrument at a heating rate of 20 ^{o}C min^{-1} in nitrogen atmosphere.

Differential scanning calorimetry (DSC). DSC traces of the polymer were obtained using a TA Q10 DSC instrument. The temperature and heat flow were calibrated using standard materials (indium and zinc) at a cooling and heating rates of 10 ^{o}C min^{-1}. The sample with a typical mass of about 5 mg was encapsulated in sealed aluminum pans.

Polarizing optical microscope (POM). LC texture of the polymer was examined under POM (Leica DM-LM-P) equipped with a Mettler Toledo hot stage (FP82HT).

One-dimensional wide-angle X-ray diffraction (1D WAXD). 1D WAXD experiments were performed on a BRUKER AXS D8 Advance diffractometer with a 40 kV FL tubes as the X-ray source (Cu Kα) and the LYNXEYE_XE detector. Background scattering was recorded and subtracted from the sample patterns. The heating and cooling rates in the 1D WAXD experiments were 10 ^{o}C min^{-1}.

Two-dimensional wideangle X-ray diffraction (2D WAXD). 2D WAXD was carried out using a BRUKER AXS D8 Discover diffractometer with a 40 kV FL tubes as the X-ray source (Cu Kα) and the VANTEC 500 detector. The point-focused X-ray beam was aligned either perpendicular or parallel to the mechanical shearing direction. For both the 1D and 2D WAXD experiments, the background scattering was recorded and subtracted from the sample patterns.

1D Small angle X-ray scattering (1D SAXS). 1D SAXS experiments were performed using a high flux SAXS instrument (SAXS ess, Anton Paar) equipped with Kratky block collimation system and a Philips PW3830 sealed tube X ray generator (Cu Kr).

Synthesis of monomer

The chemical structures and synthetic procedures of monomer (MBTC) were shown in Scheme 1. 2-Hydroxyl-3, 6, 7, 10, 11-pentakis (hexyloxy) triphenylene (PHT) was easy to obtain according our work. The experimental details were described as follows: 2-Hydroxyl-3, 6, 7, 10, 11-pentakis (hexyloxy) triphenylene (PHT) and 2-vinylterephthalic acid (VTA), were facilely synthesized via DCC condensation. PHT (3.875 g, 5.2 mmol), VTA (0.5 g, 2.6 mmol), N, N'-dicyclohexylcarbodiimide (DCC, 1.073 g, 5.2 mmol), 4-(dimethylamino) pyridine (DMAP, 0.06 g, 0.52 mmol), and dried CH_2Cl_2 (100 mL) were mixed in a 250 mL round-bottomed flask then stirred at ambient temperature for 24 h. The floating solid was filtrated, and the solvent was evaporated under reduced pressure. The crude product was purified by silica gel column chromatography with CH_2Cl_2 as eluent and subsequent recrystallization from methyl alcohol as a faint yellow powder. Yield: 48%. ^1H NMR (δ): 8.62 (d 1H, Ar-*H*), 8.37-8.35 (e 2H, Ar-*H*), 8.26-7.90 (f 2H, Ar-*H*, l 2H, Ar-*H*, m 4H, Ar-*H*, n 4H, Ar-*H*), 7.85-7.82 (c 1H, -C*H*=), 5.98-5.93 (b 1H, =C*H*$_2$), 5.54-5.51 (a 1H, =C*H*$_2$), 4.24 (g 20H, -C*H*$_2$-), 1.95 (h 20H, -C*H*$_2$-), 1.81 (i 20H, -C*H*$_2$-), 1.58 (j 40H, -C*H*$_2$-), 0.94 (k 30H, -C*H*$_3$). ^{13}C NMR (δ): 14.06 (-*C*H$_3$), 22.54-31.73 (-*C*H$_2$-), 68.89 (-O*C*H$_2$-), 115.08 (=*C*H$_2$), 123.02 (aromatic *C*-O), 123.22-124.76 (aromatic *C*), 128.20 (middle aromatic *C*), 132.71 (-H*C*=*C*H$_2$), 139.72 (aromatic *C*-H*C*=*C*H$_2$), 148.86-149.85 (aromatic *C*-O), 158.08 (aromatic *C*-O), 164.33 (*C*=O). Mass Spectrometry (MS) (m/z) [M] Calcd for $C_{106}H_{148}O_{14}$, 1645.09; found, 1645 +1.

Synthesis of polymer

As shown in Scheme 1, the polymer was synthesized by conventional solution free-radical polymerization. The detailed procedure was carried out as follows: 0.3 g (0.18 mmol) of MBTC, 100 μL of tetrahydrofuran (THF) solution of 0.01 mmol AIBN, 2 mL of THF, and a magnetic stir bar were added into a polymerization tube, the tube was purged with nitrogen and subjected to three freeze thaw cycles to remove any dissolved oxygen and sealed off under vacuum. Polymerization was performed at 75 ^{o}C for 12 h. Subsequently, the polymerization was stopped by dipping the tube in ice water. Then the tube was opened, and the reaction mixture was diluted with 10 mL of THF. The resultant polymer was precipitated and washed with methanol. To eliminate the unreacted monomers completely, the purification was repeated for three times, until no peak was observed at the elution time of monomer in gel permeation chromatography (GPC) measurement. The target polymer

poly[bis(3, 6, 7, 10, 11-pentakis (hexyloxy) triphenylen-2-yl)2-vinylterephthalate] (PBTCS) was obtained as a faint yellow solid.

Yield: 68%.

Scheme 1 Synthetic route of the polymer (PBTCS)
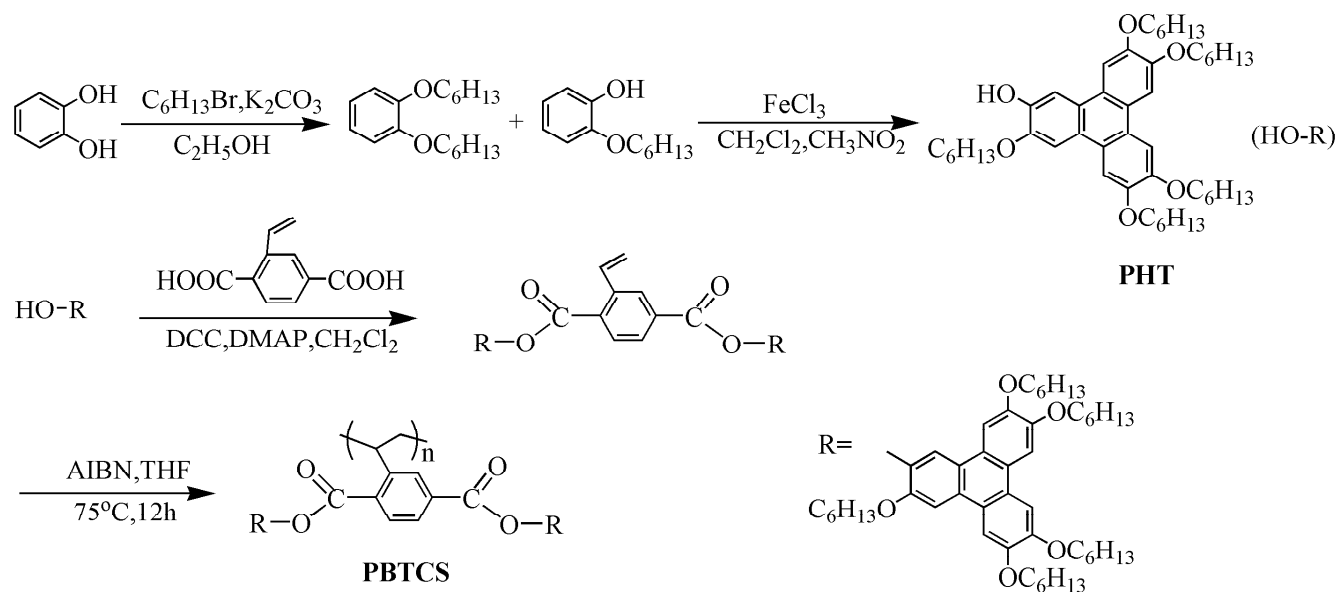
Results and discussion

Synthesis and characterization of monomer and polymer

PHT reacted with VTA via Steglich esterification to obtain the monomer. And the monomer could be easily polymerized via free radical polymerization. The molecular characterizations of the polymer were summarized in Table 1. GPC analysis of the polymer shows that a number-average weight (M_n) of the PBTCS is 1.7×10^4 g mol^{-1}, with polydispersities of 1.43, confirming good polymerizability of the monomer. The chemical structure of the monomer was confirmed by ^{1}H/^{13}C NMR and high-resolution mass spectrometry. Fig.1a and Fig.1b gives the ^{1}H NMR spectra (CDCl$_3$) of the monomer MBTC and the polymer PBTCS, respectively. The characteristic resonances of vinyl group appearing at 5.54 - 5.93 and 7.82 - 7.85 ppm completely disappear after polymerization, and the resonance peaks of PBTCS were rather broad and consistent with the expected polymer structure, indicating the successful polymerization as well.
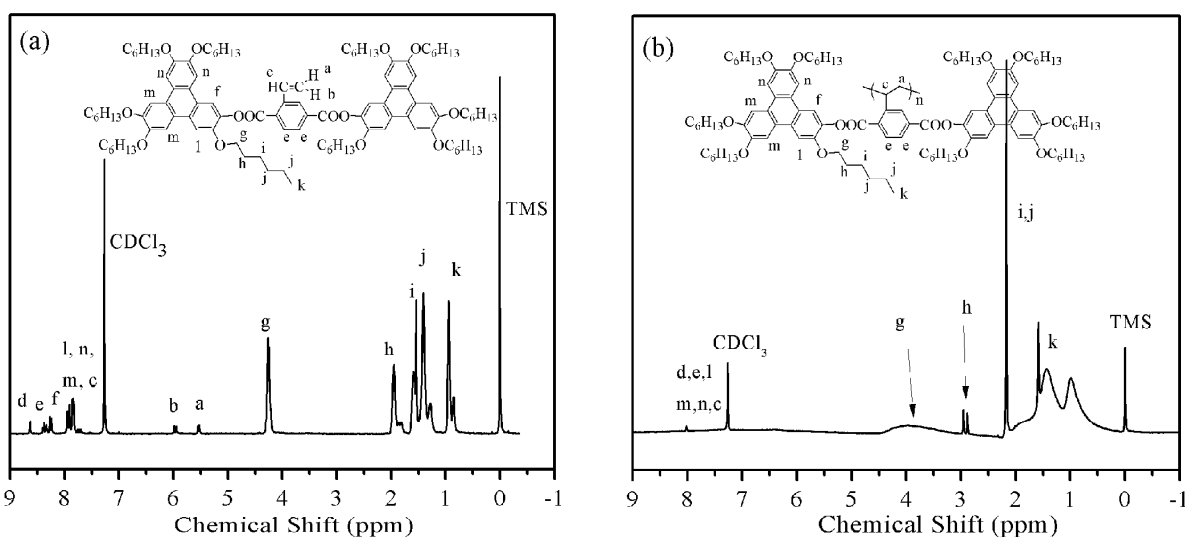
Fig.1 ^{1}H NMR spectra of monomer MBTC (a) and the polymer PBTCS (b) in CDCl$_3$

Table 1 Molecular characteristics of PBTCS

Polymer	$M_n(\times 10^{-4}$ g mol^{-1})^a	PDI^a	T_g(°C)^b	T_g(°C)^c	T_i(°C)^d	$T_d(N_2)^e$
PBTCS	1.7	1.43	217	222	285	385

a. Determined by GPC in THF using PS standards.

b. Evaluated by DSC during the first cooling process at a rate of 10 °C min^{-1}, under nitrogen atmosphere.

c. Evaluated by DSC during the second heating process at a rate of 10 °C min^{-1}, under nitrogen atmosphere.

5 d. The phase transition temperature form liquid crystalline to isotropic phase (T_i) was evaluated by POM at a heating rate of 5 °C min^{-1}.

e. The temperatures at which 5% weight loss of the sample under nitrogen [$T_d(N_2)$] was measured by TGA heating experiments at a rate of 20 °C min^{-1}.

Mesomorphic properties of the monomer

The phase behaviors of the monomer were examined by the conventional analyses including DSC and POM. In order to avoid 10 the thermal polymerization, the detection temperature of DSC and POM was below 210 °C. The thermograms of MBTC on both first cooling scans and the second heating were shown in Fig.2, and its phase transition temperatures were collected in Table 2. The results showed that the MBTC presented crystal phase in low 15 temperature (Fig.3a) and formed columnar phase when the temperature raised to 131 °C (Fig.3b). With the temperature going up, it turned into nematic phase (Fig.3c). Once the temperature reaches 204 °C, the schlieren textures disappeared, indicating entered into isotropic state, which was consisted with 20 the DSC results.
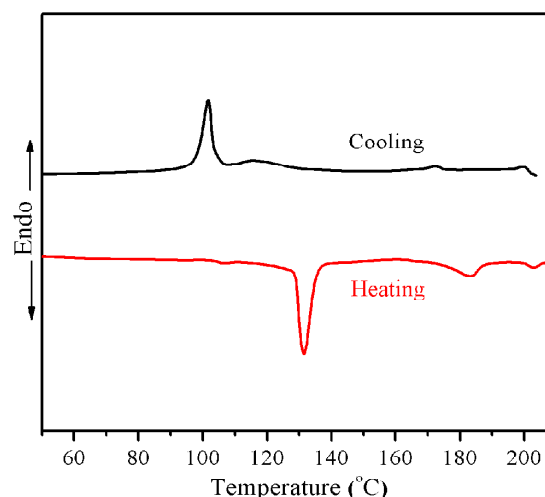
Fig.2 DSC thermogram of MBTC during the first cooling and second heating at a rate of 5 °C min-1 under nitrogen atmosphere.

25 **Table 2** Liquid-crystalline properties of the monomer

Monomer	Phase transitions (°C)	
	First cooling	Second heating
MBTC	I(201)N(172)Col(106)Cr	Cr(131)Col(178)N(204)I

Cr: crystalline; N: nematic; Col: columnar; and I: Isotropic phase.
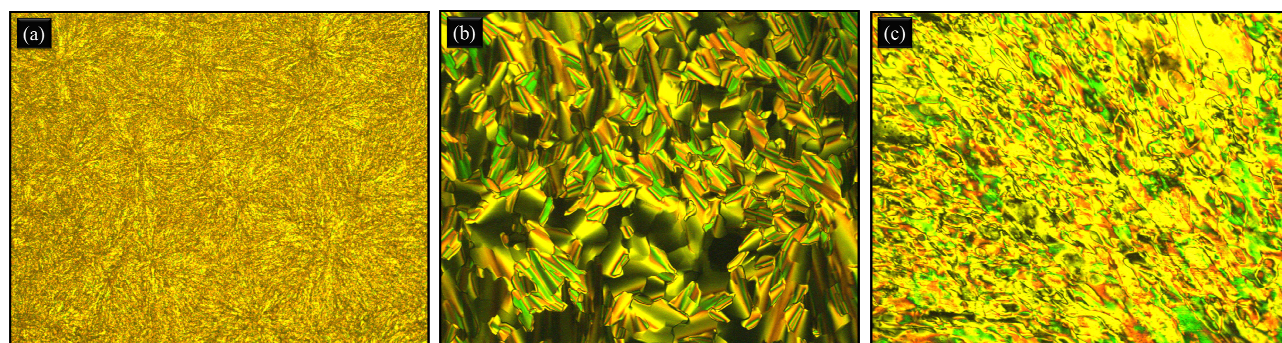
Fig.3 The representative POM images of the texture of MBTC maintained at (a) 68 °C, (b) 160 °C and (c) 190 °C (200x).

30 The phase transitions and structure of the MBTC were further veried on the 1D WAXD instrument. Fig.4 illustrates the 1D WAXD patterns of the MBTC obtained during the first heating process. As shown in Fig.4, MBTC formed the crystal structure when the temperature below 140 °C. With the temperature going 35 up, many diffraction peaks disappeared in the high 2θ range, meantime, the π - π interactions of the triphenylene was observed at ~ 25 °C, indicating that MBTC entered into the column structure. However, when the temperature raised to 180 °C, the π

- π interactions of the triphenylene was disappeared in the high 2θ range, suggesting the formation of another ordered structure. Combined the POM result (as shown in Fig.3d), the monomer exhibited the nematic phase in high temperature. At last, the diffusion peaks was observed in the low and high 2θ range, showing the isotropic phase.
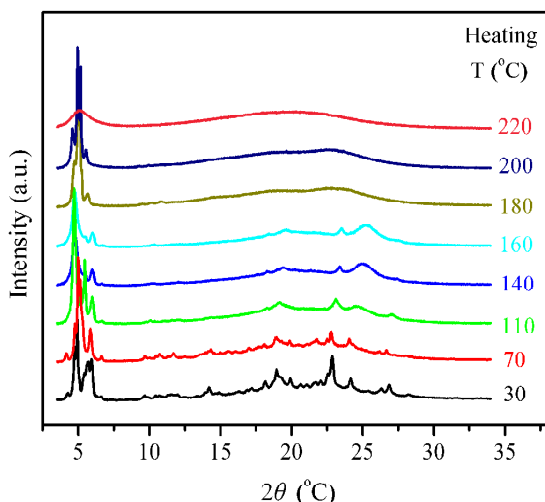
Fig.4 1D WAXD patterns of MBTC during the first heating

Thermal and liquid crystalline properties of the polymer

The thermal and liquid crystalline properties of the polymer were investigated by TGA, DSC and POM. As shown in Table 1, the polymer exhibit excellent thermal stability, with the temperatures at 5% weight loss of the sample under nitrogen was about 385 ^{o}C measured by TGA at a rate of 20 ^{o}C min^{-1}.

The phase transition behaviors of the polymer were investigated by DSC. Fig.5 shows the first cooling and the second heating DSC curves of PBTCS at a rate of 10 ^{o}C min^{-1} under nitrogen atmosphere after eliminating the thermal history. As can be seen, the glass transition temperature (T_g) of the polymer can be observed. As expected, the polymer got a relatively higher T_g (222 ^{o}C), compared to PPnV (n is the number of the methylene units between the terephthalate core and Tp moieties in the side chains). For example, when n = 3, 6, 9, the T_g of the polymers was 60 ^{o}C, 21 ^{o}C and 6 ^{o}C, respectively, indicating that the T_g decreased with the increased of the spacer.[36,37] The DSC profile of PBTCS from 50 to 250 ^{o}C shows only a glass transition step but no endothermic peak correlating to a phase transition, which is characteristic for most MJLCPs reported. Due to the insensitivity of the DSC method to determine the phase transitions of the polymer except for glass transitions, POM and WAXD techniques were utilized to further investigate PBTCS LC phase behavior.
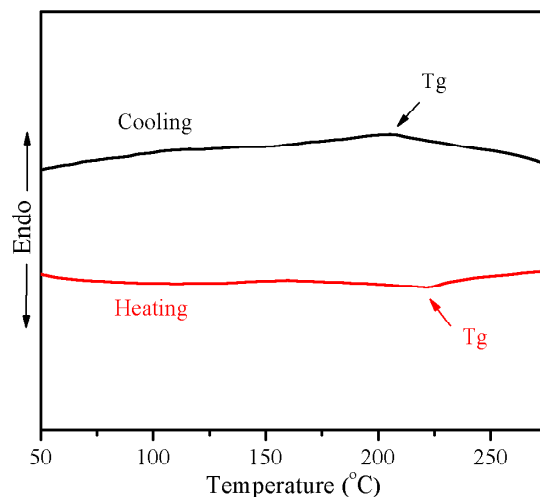
Fig.5 DSC thermogram of PBTCS during the first cooling and second heating at a rate of 10 ^{o}C min^{-1} under nitrogen atmosphere.

Birefringence of the polymer was observed by POM. The sample was cast from CH_2Cl_2 solution and slowly dried at room temperature, then slowly heated. The POM results are shown in Fig.6. As can be seen from it, the pseudo focal-conic fan textures were observed at 213 ^{o}C, which is the typical texture of columnar phase. When temperature reaches 285 ^{o}C, the birefringence disappeared and the field of vision became dark, indicating that the polymer entered into the isotropic state. When cooled to room temperature from 285 ^{o}C, the birefringence was observed again, which implying the forming of ordered structure was reversible.
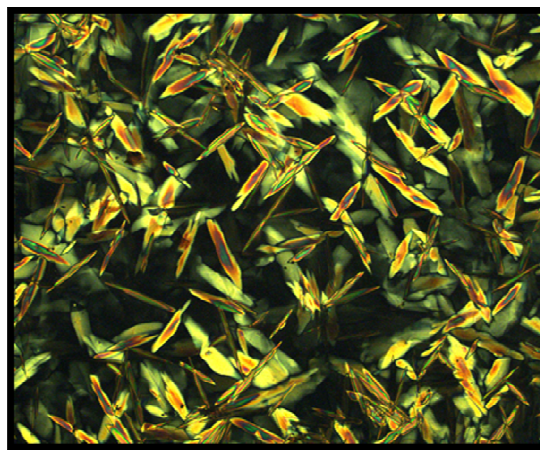
Fig.6 The representative polarized micrograph of the texture at 213 ^{o}C of PBTCS (200x).

Phase structure identification of the polymer

To identify the phase structures of PBTCS, 1D (at different temperatures) and 2D WAXD experiments were carried out. A sample for 1D WAXD experiments was about 50 mg of the polymer was added into an aluminum foil substrate. 2D WAXD pattern was recorded with the X-ray incident beam perpendicular to the shear direction. The sample was thermally annealed overnight at an appropriate temperature above T_g before 2D WAXD experiments.

1D WAXD profiles of PBTCS during the first heating and subsequent cooling processes were shown in Fig.7a and Fig.7b,

respectively. Whether the temperature lower or higher than the T_g of the polymer (222 °C), the patterns of low-angle region renders two sharp diffraction peaks, indicating the existence of an ordered structure. With heating to higher temperatures, in the low-angle region the peaks slightly shifted to lower angle and the first peak intensity increase due to thermal expansion. Two sharp peaks with a scattering vector ratio of 1: $3^{1/2}$ ($q = 4\pi\sin\theta/\lambda$, where λ is the X-ray wavelength and 2θ the scattering angle) appear, and the corresponding d-spacing values of the tow peaks are 2.74 and 1.64 nm, which indexed as the (100) and (110) diffractions, demonstrating an ordered hexagonal lattice with a = b = 3.17 nm, γ = 120°. The absence of (hkl) diffractions indicates that the polymers formed a 2D positional order, similar to many other MJLCPs.[39,40]
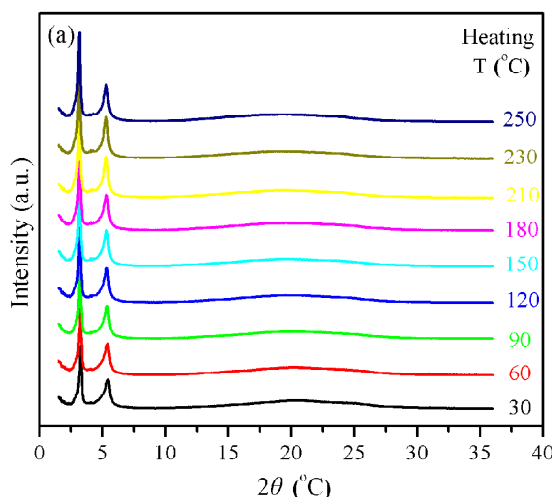
By simulated calculated, the length of the Tp moiety with all-trans conformation of C6 alkyl arms is ca. 2.3 nm. Nevertheless, the whole side chain length cannot be precisely estimated, owing to the possible rotation of the ester linkage. However, depending on the relative position of Tp moieties in the side chain, the dimension of the whole side chain should be not exceeding 4.6 nm. Meantime, in high-angle region, the broad weak peak at 2θ of ~25° indicates that there only exhibits weak π - π interactions of the side-chain triphenylene discogens (see Fig.7a). Therefore, we presume that the structure of the LC phase is hexagonal columnar (Φ_H) phase,[41,42] developed by the "jacketing effect" rod-like supramolecular mesogen, suggesting the mesogenic groups and main chain construct cylinders and the mesogenic groups were tilted ~45° away from the cylinder long axis.[43,44]
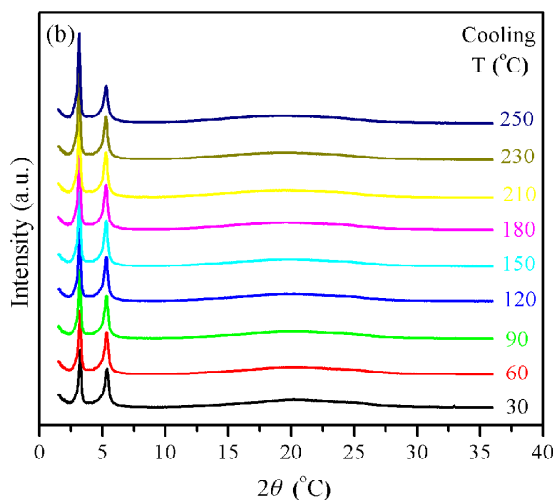
Fig.7 1D WAXD patterns of PBTCS during the first heating (a) and subsequent cooling (b)

The 1D WAXD profiles in the heating process follow much the same pathways to those in the cooling process. Fig.8 shows plots of the d-spacing of the (100) diffraction (d_{100}) against temperature. A continuous increase of d_{100} is observed during heating with no transition, as the same cannot be detected in DSC. Upon cooling, with a same continuous d-spacing decrease compared with that in the heating process, indicating the formation of the stable LC phase. Regardless of the heating process or the cooling process, the degree of order of this phase does not change much (2.72 nm to 2.80 nm).
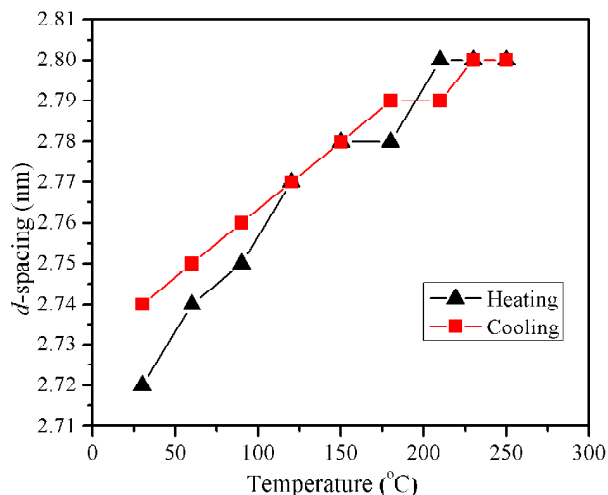
Fig.8 d-spacing values of the first diffraction peak in the 1D WAXD patterns of PBTCS during the first heating and subsequent cooling processes as a function of temperature.

In order to further elucidate the phase structure of PBTCS, we performed 1D SAXS experiment. The polymer was heated to 250 °C, and then slowly cooled to the room temperature. Fig.9 shows the 1D SAXS profiles of PBTCS. As can be seen, a first-order sharp peak is centered at $q^* = 2.23$ nm^{-1} and a secondary diffraction peak appear at $3^{1/2}q^* = 3.74$ nm^{-1}, with the ratio of q^*:

$3^{1/2}q^*$ was 1：$3^{1/2}$, indicating a hexagonal columnar structure with a periodicity of 2.81 nm ($d_{100} = 2\pi/q^*$), which is consistent with the 1D WAXD results (2.74 nm).
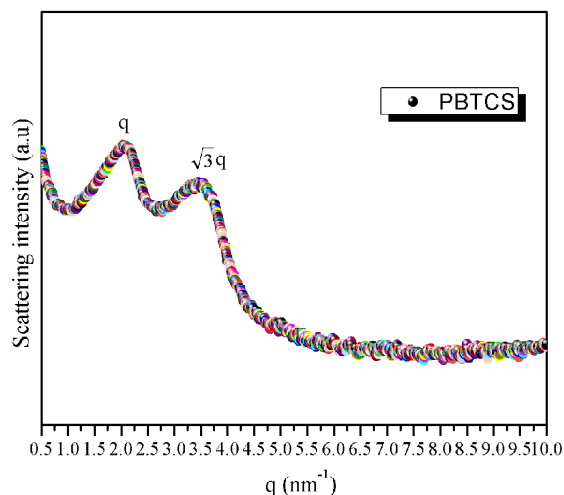
5 **Fig.9** 1D SAXS profiles of PBTCS recorded at room temperature with intensity in log scale

2D WAXD experiments were carried out to further characterize the mesomorphic phase structure of PBTCS. Fig.10a depicts the 2D WAXD pattern of PBTCS at room temperature. 10 The film sample was obtained and treated with a relatively large shear force at 250 °C. As can be seen from it, with the shear direction on the meridian, two pairs of sharp arcs appear on the equator, indicating the existence of ordered structures on the nanometer scale with lattice planes oriented primarily parallel to 15 the meridian direction. In general, the polymer chain will be oriented parallel to the direction of the shear force. Hence, the absence of the diffractions on other directions except those on the equator in the low-angle region ensured that all of the low-angle diffractions can be attributed to (hk0) diffractions. In particular, 20 when setting the sample vertically and letting X-ray beam go through x, 6-fold symmetry of the (110) diffractions can be observed, as shown in Fig.10c, which elucidate more clearly the hexagonal packing, the corresponding azimuthal intensity profile of six peaks were 31°, 91°, 152°, 214°, 274° and 335° (as shown in 25 Fig.10d). This observation is consistent with the assignment of the diffraction peaks in 1D WAXD patterns. Therefore, all Tp moieties are aligned with the polymer main chain to form a stabilized ordered phase. Therefore, the 2D WAXD patterns combining the results of POM and 1D WAXD support that 30 PBTCS possesses a 2D Φ_H phase developed by the rod-like supramolecular mesogen and main chain.
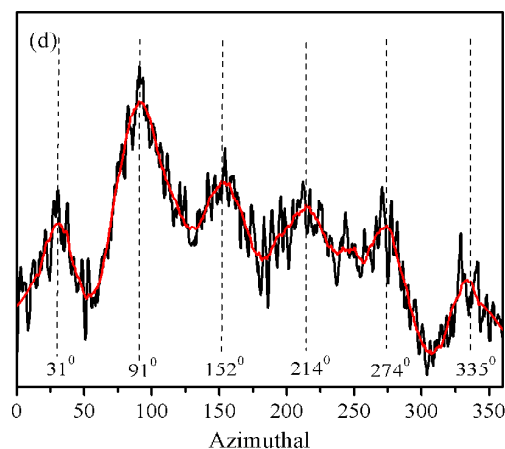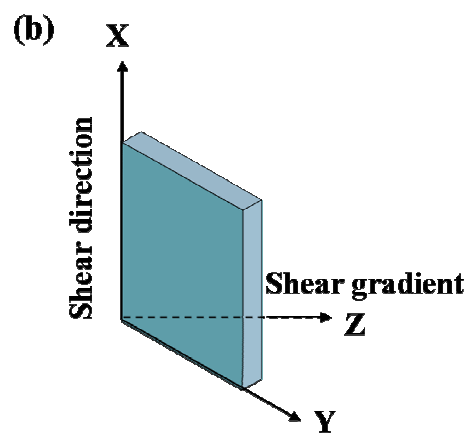
Fig.10 2D WAXD patterns of PBTCS at room temperature, with the X-ray beam perpendicular (a) and parallel (c) to the shear direction, and the shearing 35 geometry (b), where X and Z are the shear direction and shear gradient. The azimuthal scanning corresponds to the equator and the meridian (d).

In order to certify the orientation of PBTCS, the sample was heated and oriented by shearing at 250 °C, and then slowly cooled

to room temperature, and at last performed by POM. As shown in Fig.11a, after the sample was oriented by shearing, the color of the texture was not bright enough, however, the sample was rotated the sample with an angle of ~45°, the color of the texture

5 has obvious changed (Fig.11b), illustrating that the side chain Tp was perpendicular to the main chain, indicated that the oriented of the main chain as the same oriented of the shearing direction.[45]
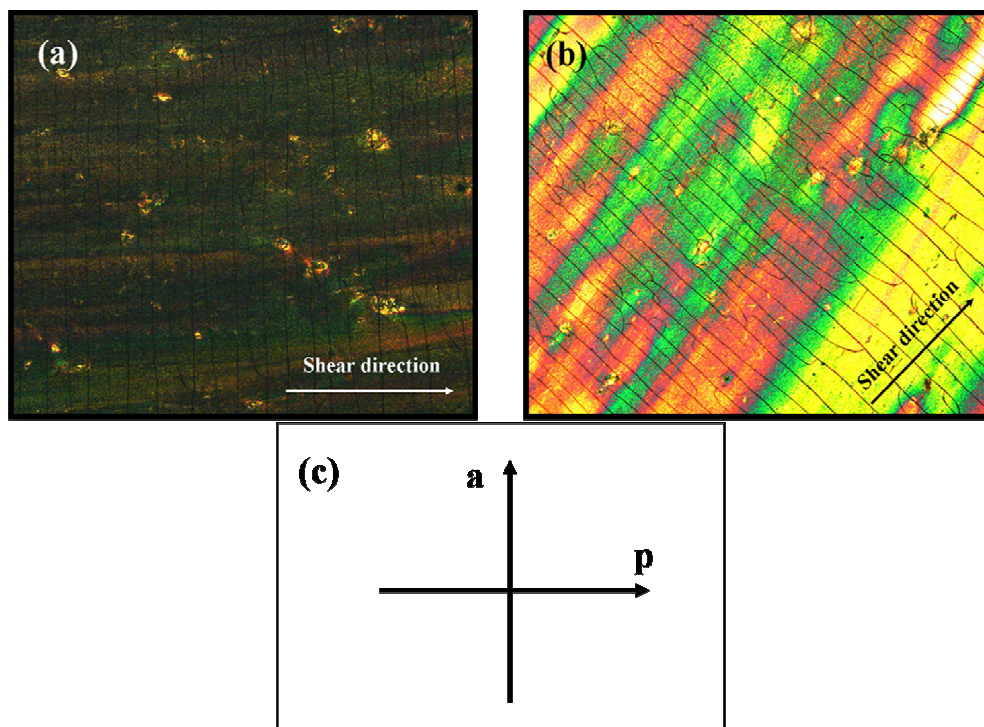
10   **Fig.11** Polarizing optical microscopic images of PBTCS prepared as follows: sheared at 250 °C. The arrows of a and p denote the directions of the analyzer and polarizer, respectively.

The reconstructed relative electron density map of PBTCS was shown in Fig.12. It is reasonable to assign the blue colored zone with low electron density to the alkyl tails of the triphenylene, the 15 red colored zone with high electron density to the triphenylene discotic mesogens, while the core (orange colored) of the column with intermediate electron density around by the red zones to the rigid backbones. The diameter of the columns in the reconstructed electron density map was well agreed with the 20 observed results by WAXD.
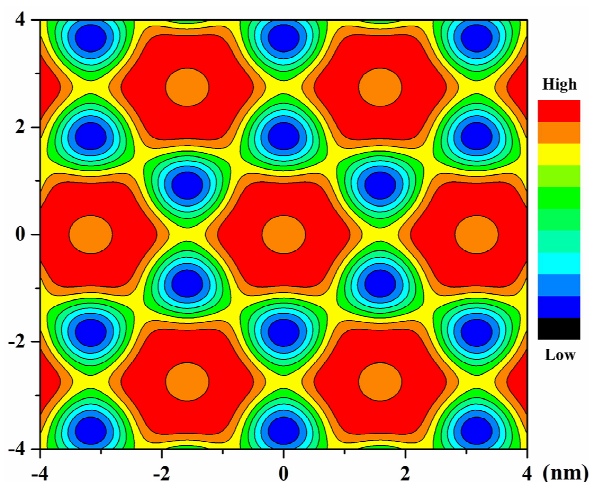
Fig.12 The reconstructed relative electron density map of the 2D hexagonal lattice of PBTCS

Fig.13 depicts a schematic drawing of the molecular packing of 25 PBTCS. From the whole tested, we found that PBTCS exhibits a stabilized phase structure, and without flexible spacer between main chain and Tp moieties in the side chains offer a stronger coupling effect, leading to overcome the π - π interaction of Tp mesgeon. As expected, without flexible spacer, the T_g of PBTCS 30 is 222 °C, which is higher than those of PPnV,[36,37] owing to the stronger steric hindrance. Meantime, PBTCS exhibited a stabilized hexagonal columnar (Φ_H) phase, whether at low or high temperature, which is different from the phase behavior of PPnV. At low temperatures, for PP3V and PP6V, both polymers formed 35 rectangular columnar (Φ_R) phases in conjunction with a discotic nematic (N_D) phase, owing to the self-organization of the Tp moieties. For PP12V, it presnted a hexagonal columnar (Φ_H) phase owing to the strong decoupling and self-organized by Tp discotic mesogens. At high temperature, PP6V formed Φ_H phase 40 and PP12V formed a Φ_N phase developed by the rod-like supramolecular mesogen - the MJLCP chain as a whole. Compared with PBTCS, PP3V and PP6V, the Tp mesgoen of PP12V showed the more ordered structure, suggesting that longer flexible spacers between MJLCP main chain and Tp moieties in 45 the side chains offered a stronger decoupling effect, which allowed for the two LC building blocks to act more independently. This result can be supported by the intensity of π - π stacking of the Tp.

The spacer length affects the interplay between the two LC 50 building blocks tremendously. Without the spacer, two Tp mesogens built like one calamitic mesogens only, therefore, the

phase behavior is similar to many other MJLCPs.[39,40] By simulated calculated, the length of two Tp moiety with all-trans conformation of C6 alkyl arms is ca. 4.6 nm. Meantime, based on experimental result, the PBTCS formed the Φ_H phase (a = b = 3.17 nm) developed by the mesogen and main chain as a whole, indicating that the mesogenic groups were tilted ∼45° away from the cylinder long axis. For PP6V, it also formed Φ_H phase (a = b = 4.35 nm) in the high temperature. But, the later polymers contained the larger a and b values compared with PBTCS, due to the increased spacer length from zero methylene units to six. For PP12V, the Tp discotic mesogens can self-organized into the Φ_H phase (a = b = 2.06 nm), owing to the strong decoupling. Simulated calculated, the length of the Tp moiety with all-trans conformation of C6 alkyl arms is ca. 2.3 nm, indicating the molecular plane of PP12V is nearly perpendicular to the formed column axis. Therefore, the spacer length has plays a very important role in the arrangement of Tp side-chain mesogens in the MJLCPs system.
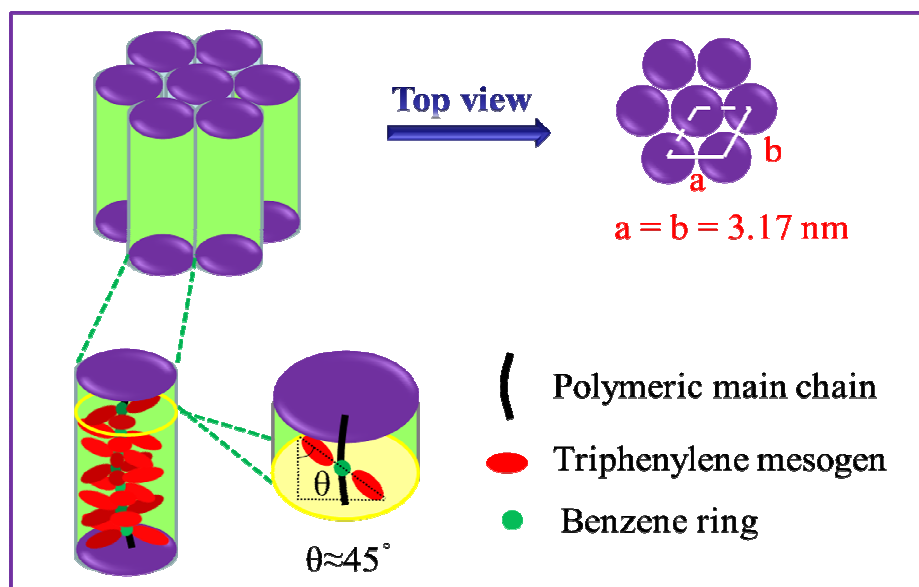
Fig.13 Schematic drawing of the PBTCS

Conclusions

In summary, using conventional free radical polymerization, we synthesized a novel MJLCP bearing Tp DLCs as pendant groups, PBTCS, with sufficiently high M_w (M_n = 1.7×10⁴ g mol⁻¹) to construct MJLCP with DLCs as the side-chain LC functional material. Combining 1D/2D WXRD and 1D SAXS results with POM and DSC observations, PBTCS exhibits a stabilized 2D Φ_H phase. As expected, when the flexible spacer is abolished, the "jacketing effect" is increased, leading to overcome the π - π interaction of Tp mesgeon. On the basis of our work, it can provide new functional materials with fine-tuning ordered structures, which is of great importance for both fundamental research and real applications.

Acknowledgments

Notes and references

1   Danli Z, Ibtissam T D, Yiming X, Farid K, Navaphun K, Martin B，Daniel G, Benoît H, Bertrand D, Dimitri A I, Emmanuelle L, David K, Fabrice M, André-Jean A. *Macromolecules*. 2014, **47**, 1715-1731.

2   Franse M W C P, te Nijenhuis K, Picken S J. *Rheol Acta*. 2003, **42**, 443-453.

3   Pal S K, Kumar S. *Liq. Cryst*. 2008, **35**, 381-384.

4   Sandeep K, Sanjay K V. *Org. Lett*. 2002, **4**, 157-159.

5   Allen M T, Diele S, Harris K D M, Hegmann T, Kariuki B M, Lose D, Preece J A, Tschierske C. *J. Mater. Chem*. 2001, **11**, 302-311.

6   Kumar, S. *Chem. Soc. Rev*. 2006, **35**, 83-109.

7   Gearba R I, Anokhin D V, Bondar A I, Bras W, Jahr M, Lehmann, M, Ivanov D A. *Adv. Mater*. 2007, **19**, 815.

8   Sergeyev S, Pisula W, Geerts Y H. *Chem. Soc. Rev*. 2007, **36**, 1902-1929.

9   Scherf U, Gutacker A, Koenen N. *Acc. Chem. Res*. 2008, **41**, 1086-1097.

10   Kouwer P H J, Jager W F, Mijs W J, Picken S J. *J. Mater. Chem*. 2003, **13**, 458-469.

11   Chen X, Chen L, Yao K, Chen Y. *ACS Appl. Mater. Interfaces*. 2013, **5**, 8321-8328.

12   Bisoyi H K, Kumar S. *J. Mater. Chem*. 2008, **18**, 3032-3039.

13   Emiliano T, Rubén C, Gerardo S E, Cesár L F, Josu O, Silverio C, Pablo E. *Inorg. Chem*. 2014, **53**, 3449-3455.

14   Julien I, Raphael M, Laurent D, Frederic C, Harald B, Yoann O, Jerome C, David B, Gabriele D'A, Otello M R, Luca M, Claudio Z. *J. Am. Chem. Soc*. 2014, **136**, 2911-2920.

15   Wu B, Mu B, Wang S, Duan J, Fang J, Cheng R, Chen D. *Macromolecules*. 2013, **46**, 2916-2929.

16   Kreuder W, Ringsdorf H. *Makromol Chem Rapid Commun*. 1983, **4**, 807-815.

17   Xing C M, Lam J W Y, Zhao K Q, Tang B Z. *J. Polym. Sci. Part A: Polym. Chem*. 2008, **46**, 2960-2974.

18   Tahar-Djebbar I, Nekelson F, Heinrich B, Donnio B, Guillon D, Kreher D, Mathevet F, Attias A J. *Chem. Mater*. 2011, **23**, 4653-4656.

19   Yu Z Q, Jacky W Y Lam, Keqing Zhao, Zhu C Z, Yang S, Lin J S, Li B S, Liu J H, Chen E Q, Tang B Z. *Polym. Chem*. 2013, **4**, 996-1005.

20 Yu Z Q, Jacky W Y L, Zhu C Z, Chen E Q, Tang B Z. *Macromolecules*. 2013, **46**, 588-596.
21 Hüser B, Spiess H W. *Macromol. Rapid. Commun*. 1988, **9**, 337-343.
22 Hüser B, Pakula T, Spiess H W. *Macromolecules*. 1989, 22, 1960-
5 1963.
23 Ringsdorf H, Wuštefeld R, Zerta E, Ebert M, Wendorff J H. *Angew. Chem, Int. Ed*. 1989, **28**, 914-918.
24 Werth M, Spiess H W. *Macromol. Rapid. Commun*. 1993, **14**, 329-338.
10 25 Boden N, Bushby R J, Lu Z B. Liq. Cryst. 1998, **25**, 47-58.
26 Imrie C T, Inkster R T, Lu Z, Ingram M D. *Mol. Cryst. Liq. Cryst*. 2004, **408**, 33-43.
27 Stewart D, S. Mchattie G, T Imrie C. *J. Mater. Chem*. 1998, **8**, 47-51.
28 Zhang D, Liu Y X, Wan X H, Zhou Q F. *Macromolecules*. 1999, **32**,
15 5183-5185.
29 Ye C, Zhang H L, Huang Y, Chen E Q, Lu Y L, Shen D Y, et al. *Macromolecules*. 2004, **37**, 7188-7196.
30 Wang X Z, Zhang H L, Chen E Q, Wang X Y, Zhou Q F. *J. Polym. Sci. Part A: Polym. Chem*. 2005, **43**, 3232-3244.
20 31 Xie H L, Hu T H, Zhang X F, Zhang H L, Chen E Q, Zhou Q F. *J. Polym. Sci. Part A: Polym. Chem*. 2008, **46**, 7310-7320.
32 Guan Y, Chen X F, Shen Z H, Wan X H, Zhou Q F. *Polymer*. 2009, **50**, 936-944.
33 Xu Y D, Yang Q, Shen Z H, Chen X F, Fan X H, Zhou Q F.
25 *Macromolecules*. 2009, **42**, 2542-2550.
34 Zhang L Y, Shen Z H, Fan X H, Zhou Q F. *J. Polym. Sci. Part A: Polym. Chem*. 2011, **49**, 3207-3217.
35 Liu Y X, Zhang D, Wan X H, Zhou Q F. *Chinese J. Polym. Sci*. 1998, **16**, 283-288.
30 36 Zhu Y F, Guan X L, Shen Z H, Fan X H, Zhou Q F. *Macromolecules*. 2012, **45**, 3346-3355.
37 Zhu Y F, Tian H J, Wu H W, Hao D Z, Zhou Y, Shen Z H, Zou D C, Sun P C, Fan X H, Zhou Q F. *J. Polym. Sci. Part A: Polym. Chem*. 2014, **52**, 295-304.
35 38 Ringsdorf H, Tschirner P, Schonherr O H, Wendorff J H. *Makromol. Chem*. 1987, **188**, 1431-1445.
39 Chen X F, Shen Z, Wan X H, Fan X H, Chen E Q, Ma Y, Zhou Q F. *Chem. Soc. Rev*. 2010, **39**, 3072-3101.
40 Xie H L, Wang S J, Zhong G Q, Liu Y X, Zhang H L, Chen E Q.
40 *Macromolecules*. 2011, **44**, 7600-7609.
41 Percec V, Bera T K, Glodde M, Fu Q, Balagurusamy V S K, Heiney P A. *Chem. Eur. J*. 2003, **9**, 921.
42 Percec V, Imam MR, Peterca M, Leowanawat P. *J. Am. Chem. Soc*. 2012, **134**, 4408.
45 43 Ye C, Zhang H L, Huang Y, Chen E Q, Lu Y L, Shen Y L, Wan X H, Shen Z H, Cheng S Z D, Zhou Q F. *Macromolecules*. 2004, **37**, 7188-7196.
44 Li C Y, Tenneti K K, Zhang D, Zhang H, Wan X, Chen E Q, Zhou Q F, Carlos A O, Igos S, Hsiao B S. *Macromolecules*. 2004, **37**, 2854-
50 2860.
45 Zhang L Y, Shen Z H, Fan X H, Zhou Q F. *J. Polym. Sci. Part A: Polym. Chem*. 2011, **49**, 3207-3217.